

## Porphyrin-[(*E*)-1,2-Diethynylethene] Scaffolding: Synthesis and Optical and Electrochemical Properties of Multinanometer-Sized Porphyrin Arrays

by Jennifer Wytko, Volker Berl, Mark McLaughlin, Rik R. Tykwinski, Martin Schreiber, and François Diederich\*

Laboratorium für Organische Chemie, ETH-Zentrum, Universitätstrasse 16, CH-8092 Zürich

and Corinne Boudon, Jean-Paul Gisselbrecht, and Maurice Gross

Laboratoire d'Electrochimie et de Chimie Physique du Corps Solide U.M.R. au C.N.R.S. n° 7512, Faculté de Chimie, Université Louis Pasteur, 1 et 4 rue Blaise Pascal, F-67008 Strasbourg Cedex

Two series of linearly conjugated hybrid materials, consisting of (*E*)-1,2-diethynylethene (DEE; hex-3-ene-1,5-diyne) and Zn<sup>II</sup> porphyrin components, were prepared by Pd<sup>0</sup>-catalyzed cross-coupling reactions. In one series, one or two DEE substituents were introduced into the *meso*-positions of the Zn<sup>II</sup> porphyrins, leading from **5**·Zn, to **9** and **1** (Scheme 1). The second series contains the linearly  $\pi$ -conjugated molecular rods **1**–**3** that span a length range from 23 Å (**1**) to 53 Å (**3**) (Fig. 1). The larger rods **2** and **3** consist of two or three porphyrin moieties, respectively, that are bridged at the *meso*-positions by *trans*-enediynediyl (hex-3-ene-1,5-diyne-1,6-diyl) linkers (Scheme 2). The UV/VIS spectra in the series **5**·Zn, **9**, and **1** (Fig. 2) showed a strong bathochromic shift of both *Soret* and *Q* bands of the Zn<sup>II</sup> porphyrin as a result of the addition of DEE substituents. Upon changing from **1** to **2** (Fig. 3), the *Q* band was further bathochromically shifted, whereas the *Soret* band remained nearly at the same position but became broadened and displayed a shoulder on the lower-wavelength edge as a result of excitonic coupling. The close resemblance between the UV/VIS spectra of **2** and **3** suggests that saturation of the optical properties in the oligomeric series already occurs at the stage of dimeric **2**. Stationary voltammetric investigations showed that the DEE substituents act as strong electron acceptors which induce large anodic shifts in the first reduction potential upon changing from **5**·Zn to **9** ( $\Delta E = 190$  mV) and to **1** ( $\Delta E = 340$  mV). Increasing the number of porphyrin moieties upon changing from **1** to **2** had no effect on the first reduction potential yet the first oxidation potential was substantially lowered ( $\Delta E = 110$  mV). Large differences in the potentials for one-electron oxidation of the two porphyrin moieties in **2** ( $\Delta E = 200$  mV) confirmed the existence of substantial electronic communication between the two macrocycles across the *trans*-enediynediyl bridge.

**1. Introduction.** – Monodisperse linearly  $\pi$ -conjugated oligomers serve as excellent models to provide specific information concerning the structural, electronic, and optical properties of their corresponding polydisperse long-chain polymeric analogs [1]. A further interest in these compounds arises from their potential to act as molecular-scale electronic and optical devices [2]. Porphyrins are appealing building blocks for the modular construction of  $\pi$ -conjugated oligomers and polymers since they offer a variety of desirable features such as rigidity, high stability, intense electronic absorptions across a wide spectral range, strong fluorescence emission, and the possibility to tailor optical and redox properties by complexation with various metal ions. Linear multinanometer-sized multiporphyrin assemblies have been prepared with the aim of modeling photosynthetic reaction centers and studying photoinduced energy and electron-transfer processes [3] (for recent examples, see [4]) or for potential electronic and photonic applications [5]. Among the various spacers employed to

bridge porphyrins in these arrays, acetylenes are particularly attractive [2a][6][7]. They rigorously define linear geometries of the covalent assemblies and ensure efficient  $\pi$ -electron conjugation between individual porphyrin chromophores. Porphyrin assemblies with alkyne-containing bridges have shown promise as molecular photonic wires [8], nonlinear optical (NLO) materials [7b][9], or molecular switches [10].

We have recently reported the construction of a series of molecular wires by oxidative *Glaser-Hay* oligomerization of (*E*)-1,2-diethynylethene (DEE; hex-3-ene-1,5-diyne) monomers with two (*t*-Bu)Me<sub>2</sub>SiOCH<sub>2</sub> side chains attached to the central olefinic bond [11]. These poly(triacetylene) (PTA) oligomers [12] displayed high stability and solubility, as well as interesting third-order NLO properties. For the preparation of conjugated molecular rods with further enhanced properties, we became interested in hybrid systems in which Zn<sup>II</sup> porphyrin moieties are interlinked by such DEE units. Here, we report the synthesis and optical and electrochemical properties of the porphyrin-DEE hybrid systems **1–3** which extend in length from 23 to 53 Å [13] (*Fig. 1*).

**2. Results and Discussion.** – 2.1. *Synthesis of the Porphyrin-DEE Hybrid Rods.* The synthesis of *meso*-alkynylated porphyrins commonly is achieved by Pd-catalyzed cross-coupling of halogenated porphyrins with terminal alkynes [3b][14]. Other methods involve the condensation of propynal derivatives with pyrroles or di(2-pyrryl)methanes [7a][15], or the formylation of the porphyrin followed by transformation of the formyl into ethynyl substituents [16]. We planned the synthesis of **1–3** by cross-coupling between appropriate DEE derivatives [11] and *meso*-diphenyl-Zn<sup>II</sup>-porphyrins bearing halide substituents in the two residual *meso*-positions. With the (*t*-Bu)Me<sub>2</sub>SiOCH<sub>2</sub> substituents on the DEE moieties and the 3-(ethoxycarbonyl)propoxy side chains on the *meso*-phenyl rings, **1–3** were expected to display sufficient solubility for investigation of their physical properties in solution.

The synthesis of the porphyrin components started with 4-(4-formylphenoxy)butanoate **4** which was prepared in 87% yield by treatment of *p*-hydroxybenzaldehyde with ethyl 4-bromobutyrate and NaH (*Scheme 1*) [17]. Condensation of **4** with di(2-pyrryl)methane [18] gave a porphyrinogen [19] that was oxidized with 2,3-dichloro-5,6-dicyano-1,4-benzoquinone (DDQ) to afford **5** (44%). Metalation of **5** with Zn(OAc)<sub>2</sub> · 2H<sub>2</sub>O in refluxing CHCl<sub>3</sub>/MeOH yielded **5** · Zn in 92% yield. Iodination of **5** to give diiodoporphyrin **6** was achieved in 90% yield with an excess of (AcO)<sub>2</sub>IPh and I<sub>2</sub> [14a] in CHCl<sub>3</sub> containing pyridine. Iodination occurred selectively at the two free *meso*-positions with no evidence of  $\beta$ -substitution. Subsequent metalation with Zn(OAc)<sub>2</sub> · 2 H<sub>2</sub>O in refluxing CHCl<sub>3</sub>/MeOH/THF provided **6** · Zn (83%). Metalation was necessary to prevent complexation of Cu or Pd by the porphyrin in the subsequent cross-coupling step. It also greatly increased the solubility of the porphyrin: in contrast to the corresponding free base porphyrin, **6** · Zn was readily soluble in THF due presumably to the weak axial coordination of this solvent to the complexed Zn<sup>II</sup> ion.

Pd-Catalyzed cross-coupling ([Pd<sub>2</sub>(dba)<sub>3</sub>], AsPh<sub>3</sub>, CuI, Et<sub>3</sub>N (dba = dibenzylideneacetone)) of **6** · Zn with mono(alkyne-protected) DEE **7** [11][20] (2.4 equiv.) afforded **1** in 60% yield. Small amounts of the monoalkynylated Zn<sup>II</sup>-porphyrins **8**

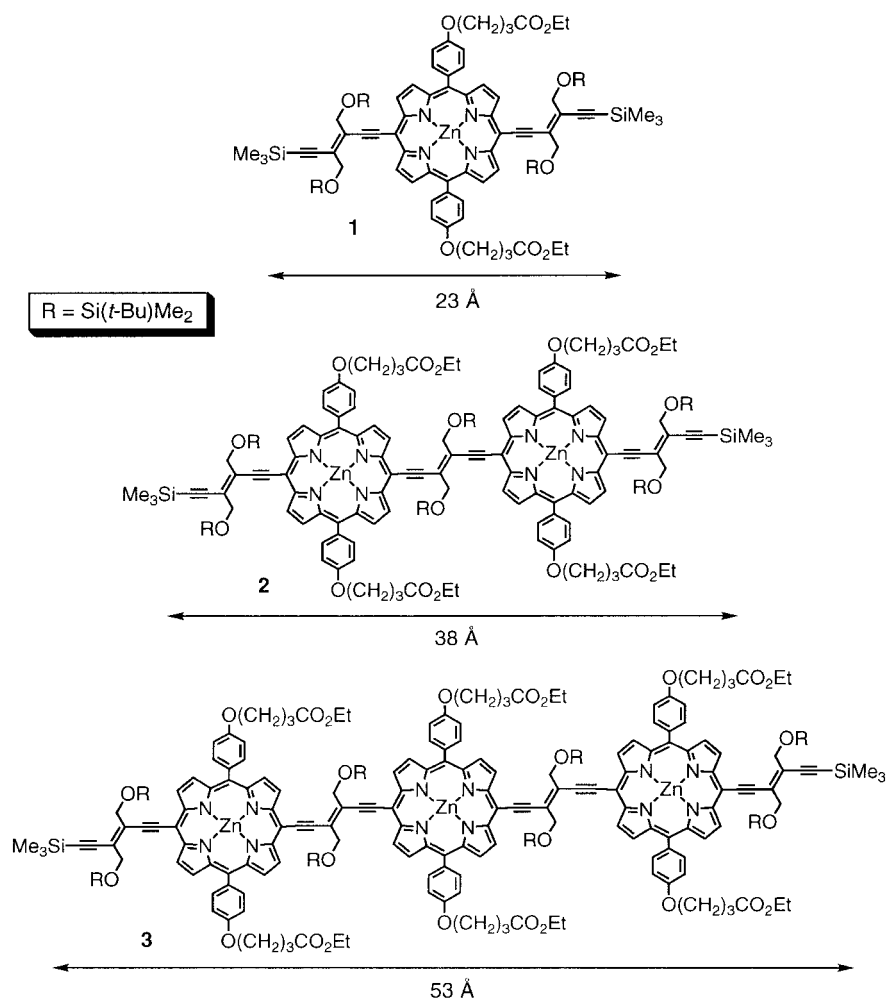
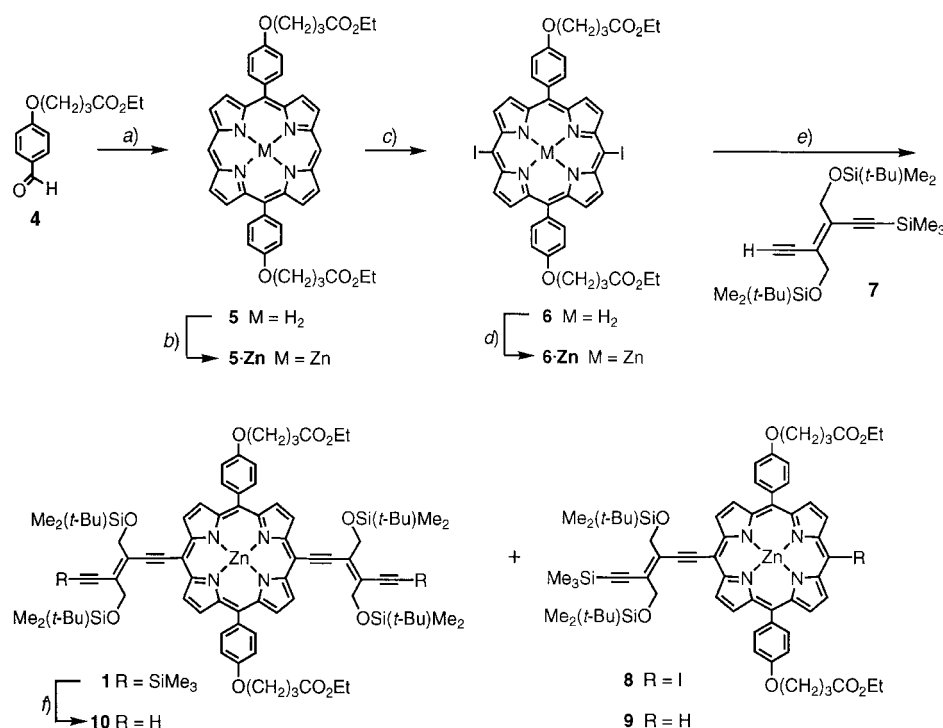


Fig. 1. Porphyrin-DEE hybrid molecular rods. The calculated rod lengths shown [11] are the distances between the Si-atoms of the terminal Me<sub>3</sub>Si groups.

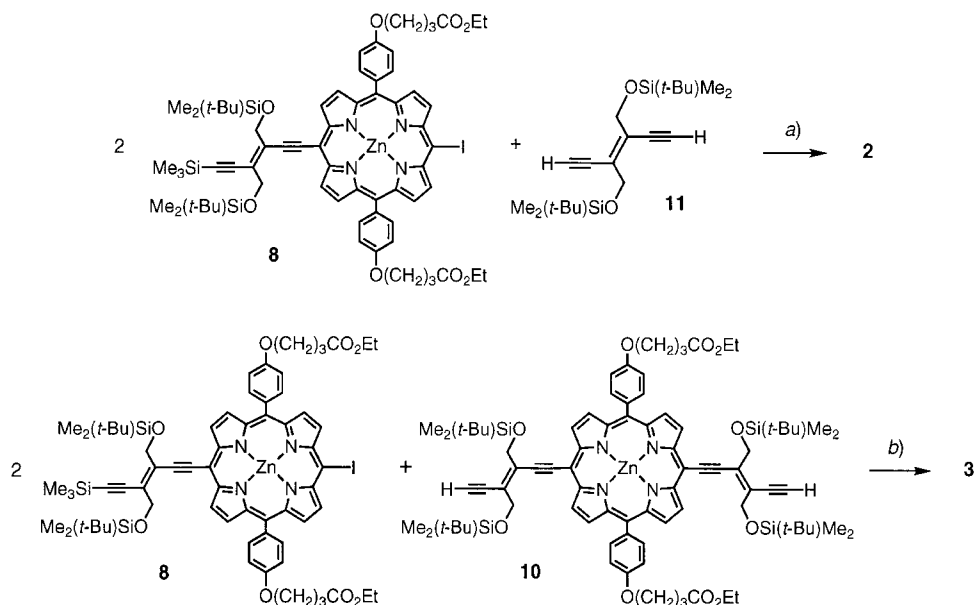
(6%) and **9** (6%) were also isolated, with the latter compound apparently originating from partial reductive elimination of iodide from the porphyrin nucleus during the catalytic cycle. The deep-green bis-DEE-appended Zn<sup>II</sup>-porphyrin **1** was separated from **8** and **9** by gel-permeation chromatography (GPC; *Biobeads SX-1*, CH<sub>2</sub>Cl<sub>2</sub>), whereas **8** and **9** could be separated by preparative TLC (SiO<sub>2</sub>; CH<sub>2</sub>Cl<sub>2</sub>/THF 99.75:0.25). The reduced product **9** later proved valuable for comparison in the UV/VIS and electrochemical investigations. Removal of the terminal alkyne-protecting Me<sub>3</sub>Si groups in **1** to give **10** was accomplished in 85% yield by conversion with AgNO<sub>3</sub> in H<sub>2</sub>O/THF/acetone to form the silver acetylide followed by alkyne demetalation with aqueous KCN solution [21]. Protodesilylation with K<sub>2</sub>CO<sub>3</sub> in MeOH/THF did not give a clean deprotection of **1** due to partial transesterification.

Scheme 1. Synthesis of the Porphyrin-DEE Hybrid Molecular Rod **1**

a) Di(2-pyrryl)methane,  $CF_3COOH$ ,  $CH_2Cl_2$ ,  $N_2$ ,  $20^\circ$ , 12 h, then 2,3-dichloro-5,6-dicyano-1,4-benzoquinone (DDQ), 20 min; 44%. b)  $Zn(OAc)_2 \cdot 2 H_2O$ ,  $CHCl_3/MeOH$ ,  $\Delta$ , 2 h; 92%. c)  $(AcO)_2IPh$ ,  $I_2$ ,  $CHCl_3$ , pyridine,  $20^\circ$ , 2 h; 90%. d)  $Zn(OAc)_2 \cdot 2 H_2O$ ,  $CHCl_3/MeOH/THF$ ,  $\Delta$ , 3 h; 83%. e)  $[Pd_2(dba)_3]$ ,  $AsPh_3$ ,  $CuI$ ,  $NEt_3$ ,  $THF$ ,  $N_2$ ,  $45^\circ$ , 6 h, then  $20^\circ$ , 12 h; 60% (**1**), 6% (**8**), and 6% (**9**). f)  $AgNO_3$ ,  $H_2O/acetone/THF$ ,  $20^\circ$ , 2 h, then  $KCN$ ,  $2$  h; 85%.

For the preparation of the longer rod **2**, iodoporphyrin **8** (2 equiv.) was subjected to Pd-catalyzed cross-coupling with DEE **11** [11][12] to yield **2** in 24% yield after several purifications by GPC and column chromatography ( $SiO_2$ ) (Scheme 2). The structure of **2** was confirmed by its  $^1H$ - and  $^{13}C$ -NMR spectra and by the FAB- and MALDI-TOF mass spectra which depicted the molecular ion at  $m/z$  2802.2 (FAB; calc. for  $^{13}C^{12}C_{153}H_{196}N_8O_{18}Si_8^{68}Zn^{64}Zn$ : 2802.1) as the parent ion. As a characteristic feature, the NMR spectrum depicted distinct resonances for three different  $(t-Bu)Me_2SiOCH_2$  groups. In the  $^1H$ -NMR spectrum, the *singlet* for the  $CH_2$  protons of the DEE moiety connecting the two porphyrins appeared significantly downfield (5.49 ppm) from the resonances of the  $CH_2$  protons (4.95 and 4.97 ppm) in the two external DEE units, in agreement with the exposure of the central  $CH_2$  protons to the deshielding anisotropic regions of two porphyrin macrocycles.

Upon Pd-catalyzed cross-coupling of **10** with 2 equiv. of **8**, the longest rod **3** was obtained as a brown-green solid in 6% yield after GPC. The MALDI-TOF mass spectrum displayed the molecular ion at  $m/z$  3950.6 (calc. for  $^{13}C^{12}C_{216}H_{268}N_{12}O_{26}Si_{10}^{68}Zn^{66}Zn^{64}Zn$ : 3949.6) as the parent ion. The  $^1H$ -NMR spectrum displayed the

Scheme 2. Synthesis of the Porphyrin-DEE Hybrid Molecular Rods **2** and **3**

a)  $[\text{Pd}_2(\text{dba})_3]$ ,  $\text{AsPh}_3$ ,  $\text{CuI}$ ,  $\text{HN}(\text{i-Pr})_2$ , THF,  $\text{N}_2$ ,  $40^\circ$ , 6 h, then  $20^\circ$ , 18 h; 24%. b)  $[\text{Pd}_2(\text{dba})_3]$ ,  $\text{AsPh}_3$ ,  $\text{CuI}$ ,  $\text{NEt}_3$ , THF,  $\text{N}_2$ ,  $20^\circ$ ; 6%.

correct number of signals for the  $\beta$ -protons of the three porphyrin nuclei and for the protons of the *meso*-phenyl rings. Furthermore, four distinct *singlets* were visible for the *t*-Bu groups of the four different  $(\text{t-Bu})\text{Me}_2\text{SiOCH}_2$  side chains at the DEE moieties. On the other hand, only two sets of three resonances appeared for the  $\text{CH}_2\text{O}$  and  $\text{MeSiO}$  groups of these side chains. The  $^{13}\text{C}$ -NMR spectrum also displayed four signals for each of the two C-atoms of the *t*-Bu groups as well as two sets of three signals for the  $\text{CH}_2\text{O}$  groups and  $\text{MeSiO}$  groups, respectively.

**2.2. Electronic Absorption Spectroscopy.** Previous work had shown that *meso*-alkynylation of metalloporphyrins resulted in large red shifts of the entire electronic absorption spectrum as a consequence of an extension of  $\pi$ -conjugation [3][5a,b][6b–d][7][9]. Attaching DEE moieties to the porphyrin skeleton imparts spectral shifts that follow this same trend (*Fig. 2* and *Table 1*). In both mono- and bis-DEE-substituted  $\text{Zn}^{\text{II}}$ -porphyrins **9** and **1**, the *Soret* bands are broadened and bathochromically shifted by 31 and 44 nm, respectively, compared to **5**·**Zn**. Even larger shifts of 45 and 93 nm were observed for the lowest energy *Q* bands of **9** and **1**, respectively, which is consistent with a decrease of the HOMO-LUMO gap. Furthermore, these low-energy  $\pi$ - $\pi^*$  transitions of **9** ( $\lambda_{\text{max}} = 625 \text{ nm}$ ,  $\epsilon = 20200 \text{ M}^{-1} \text{ cm}^{-1}$ ) and **1** ( $\lambda_{\text{max}} = 673 \text{ nm}$ ,  $\epsilon = 70100 \text{ M}^{-1} \text{ cm}^{-1}$ ) are significantly more intense than the corresponding absorption in **5**·**Zn** ( $\lambda_{\text{max}} = 580 \text{ nm}$ ,  $\epsilon = 2800 \text{ M}^{-1} \text{ cm}^{-1}$ ). With increasing number of DEE substituents,  $\pi$ -electron delocalization is substantially enhanced.

As the rod size increases from **1** to **2** and **3**, both the *Soret* and the *Q* bands become significantly broadened (*Fig. 3*). The spectra of the extended rods **2** and **3**, with two and

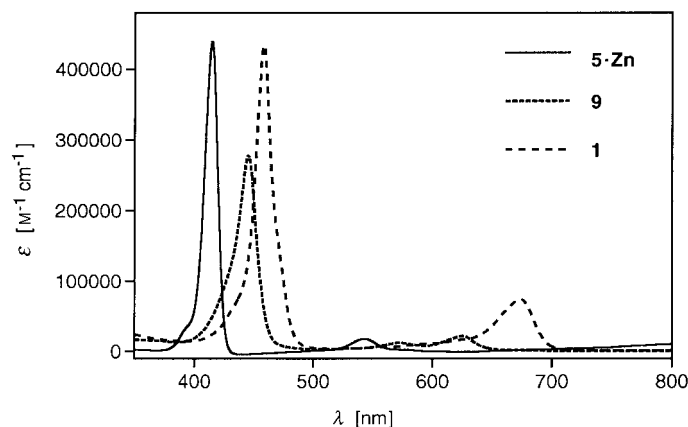


Fig. 2. Electronic absorption spectra ( $\text{CHCl}_3$ , 293 K) of  $\text{Zn}^{\text{II}}$ -porphyrins containing zero, one, and two DEE substituents in the meso-positions

Table 1. Electronic Absorption Bands of Porphyrin-DEE Hybrid Systems in  $\text{CHCl}_3$

Compound	Soret Band Region		Q Band Region	
	$\lambda_{\text{max}}$ [nm]	$\epsilon$ [ $\text{M}^{-1} \text{cm}^{-1}$ ]	$\lambda_{\text{max}}$ [nm]	$\epsilon$ [ $\text{M}^{-1} \text{cm}^{-1}$ ]
<b>5·Zn</b>	414	439100	479 (sh)	1000
			508 (sh)	2500
			543	17600
			580	2800
<b>9</b>	445	277800	535 (sh)	4000
			572	11600
			625	20200
<b>1</b>	458	426100	560 (sh)	4900
			596 (sh)	9400
			624 (sh)	14800
			673	70100
<b>2</b>	460	156600	592	18600
			650 (sh)	38100
	511 (sh)	56600	696	66900
			726	69100
<b>3</b>	457	315300	588	26800
			496 (sh)	150000
			730	111800

three porphyrin moieties connected by DEE linkers, respectively, resemble each other rather closely. With increasing  $\pi$ -electron conjugation length, the lowest energy  $Q$  band in **2** is bathochromically shifted by 53 nm (*ca.* 0.1 eV) as compared to **1**. The maxima of the *Soret* peaks in **1** ( $\lambda_{\text{max}} = 458$  nm) and **2** ( $\lambda_{\text{max}} = 460$  nm) appear at nearly the same wavelength. In addition, a shoulder appears at the lower-energy edge of the *Soret* band in **2**. Overall, the introduction of the second porphyrin moiety in **2** and the corresponding increase in overall size of the linearly conjugated  $\pi$ -chromophore affects the position of the  $Q$  band much more strongly than that of the *Soret* band.

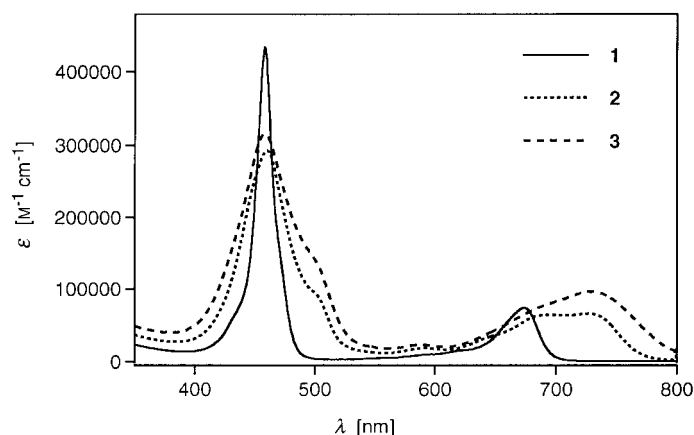


Fig. 3. Electronic absorption spectra ( $\text{CHCl}_3$ , 293 K) of the porphyrin-DEE hybrid molecular rods **1–3**

The *Soret* band in **2** spans a wide wavelength range between *ca.* 420 and 520 nm. Based on the theory of excitonic coupling of proximate chromophores by *Kasha et al.* [22], we assign the strong peak at 460 nm to the *x*-polarized transition and the shoulder at the lower-energy edge to the *y*-polarized one. In other alkyne-linked dimeric porphyrins [3][5a,b][6e][7], a weaker *y*-polarized transition usually appeared blue-shifted relative to the *x*-polarized one.

The shape of the *Soret* band in **2**, in which the two macrocyclic chromophores are linked by a (*t*-Bu) $\text{Me}_2\text{SiOCH}_2$ -substituted *trans*-enediyne ( $-\text{C}\equiv\text{C}-\text{CR}=\text{CR}-\text{C}\equiv\text{C}-$ ) bridge, differs considerably from that reported by *Arnold* and *James* for a very similar dimeric rod, in which an unsubstituted *trans*-enediyne ( $-\text{C}\equiv\text{C}-\text{CH}=\text{CH}-\text{C}\equiv\text{C}-$ ) bridge links together two  $\text{Ni}^{\text{II}}$ -octaethylporphyrins [5b]. The UV/VIS spectrum of the latter compound in  $\text{CHCl}_3$  displays a much broader *Soret* band which, in addition, is distinctly split. Based on investigations by *Anderson et al.* [7], we tentatively explain the different shape of the *Soret* band in the two dimeric systems by differences in aggregation behavior. Although it was not reported by *Arnold* and *James* whether their dimer aggregates in the concentration ranges of the UV/VIS studies [5b],  $\pi$ -stacking seems highly probable based on the findings by *Anderson et al.* for buta-1,3-diyne-linked dimeric  $\text{Zn}^{\text{II}}$ -porphyrins [7]. In contrast, the bulky (*t*-Bu) $\text{Me}_2\text{SiOCH}_2$  groups in the hex-3-ene-1,5-diyne-1,6-diyl linker prevent aggregation of **2** as confirmed by UV/VIS dilution studies. In an aggregate, the two porphyrins are fixed in a coplanar orientation, whereas, in the monodisperse form, their planes may adopt all possible torsional angles, and such geometric differences may affect the excitonic coupling and the shape of the *Soret* band<sup>1)</sup>.

The electronic absorption spectrum of trimeric **3** (Fig. 3) is very similar to that of dimeric **2**. The position of the *Soret* band is unchanged and the lowest-energy *Q* band is

<sup>1)</sup> A linear polymeric system, in which the *meso*-positions of adjacent porphyrin units are connected by  $-\text{C}\equiv\text{C}-p\text{-C}_6\text{H}_4-\text{C}\equiv\text{C}-$  linkers, while bulky mesityl residues in the two remaining *meso*-positions prevent  $\pi$ -stacking, displays a *Soret* band similar to that of **2**, with the shoulder at the lower-energy edge; see [6b].

red-shifted by a mere 4 nm ( $\lambda_{\max} = 730$  nm) relative to the same transition in **3** ( $\lambda_{\max} = 726$  nm). The major difference between the spectra of **2** and **3** is the higher intensity of the *Q* band ( $\epsilon[\text{M}^{-1} \text{cm}^{-1}] = 111800$  for **3** vs. 69100 for **2**). This effect is simply due to the increased number of DEE-substituted porphyrin subunits in **3**. The negligible bathochromic shift of the *Q* band, as compared to **2**, suggests that a saturation of the optical properties has already nearly been reached, *i.e.*, the longest wavelength maximum and the optical gap will not further change with increasing oligomeric length.

2.3. *Electrochemistry.* Stationary and cyclic voltammetric investigations were carried out on a glassy carbon working electrode in  $\text{CH}_2\text{Cl}_2$  (+0.1M  $\text{Bu}_4\text{NPF}_6$ ). Compounds **5**·**Zn**, **9**, and **1** showed two one-electron oxidation and two one-electron reduction waves (Table 2), all of which were porphyrin-based. Whereas all three compounds were reversibly oxidized at similar potentials, reductions became substantially facilitated upon increasing DEE substitution. Thus, the first reduction step was anodically shifted from  $-1.85$  V in **5**·**Zn** to  $-1.66$  V in **9** ( $\Delta E = 190$  mV) and to  $-1.50$  mV in **1** ( $\Delta E = 350$  mV). These shifts are remarkable in that they demonstrate the highly electron-deficient nature of the DEE moieties. The electron-withdrawing effect of a *meso*-DEE substituent on a porphyrin is actually equivalent to that of a thiocyanate attached to a porphyrin at a  $\beta$ -C-atom [23]. A more appropriate comparison with the influence of electron-withdrawing substituents in the *meso*-position on the reduction potentials of  $\text{Zn}^{\text{II}}$ -porphyrins can, unfortunately, not be made since such data are, to the best of our knowledge, not available<sup>2)</sup>. The ease of reduction of **9** and **1** reflects a significant lowering in energy of the LUMOs (*lowest unoccupied molecular orbital*) induced by a decrease in electron density of the porphyrin core upon functionalization with the electron-withdrawing DEE groups. Since the first oxidation potential hardly changes in the series, the lowering of the LUMO energy leads to a significant decrease in the HOMO-LUMO gap (HOMO = *highest occupied molecular orbital*), determined as the difference of the first oxidation and first reduction potentials. This electrochemical gap becomes reduced from 2.22 V in **5**·**Zn** to 1.86 V in **1**. These data are quite consistent with the optical solution gaps  $E_g$ , approximated by the maximum of the lowest-energy absorption band (Table 2).

Table 2. Redox Characteristics of Porphyrin-DEE Hybrid Systems Determined by Stationary Voltammetry on a Glassy Carbon Working Electrode in  $\text{CH}_2\text{Cl}_2 + 0.1\text{M Bu}_4\text{NPF}_6$  at  $0.1 \text{ V s}^{-1}$

Compound	$E_1^{\text{Red a}}$	$E_2^{\text{Red a}}$	$E_1^{\text{Ox a}}$	$E_2^{\text{Ox a}}$	$E_1^{\text{Ox}} - E_1^{\text{Red b}}$	$E_g (\lambda_{\max})$
<b>5</b> · <b>Zn</b>	$-1.85$ (70)	$-2.27$ (70)	$+0.37$ (58)	$+0.71$ (55)	2.22	2.14
<b>9</b>	$-1.66$ (85)	$-2.10$ (66)	$+0.35$ (62)	$+0.70$ (68)	2.01	1.98
<b>1</b>	$-1.50$ (100)	$-1.96$ (90)	$+0.36$ (71)	$+0.75$ (58)	1.86	1.84
<b>2</b>	$-1.50$ (140)	$-2.10$ (150)	$+0.25/$ $+0.45$ (200)	$+0.82$	1.75	1.71

<sup>a)</sup> V vs. Fc/Fc<sup>+</sup>; in parenthesis, slope  $\log[I(I_d - I)]$  [mV]. <sup>b)</sup> Electrochemical gap [V]. <sup>c)</sup> Optical solution gap [eV] approximated from the longest wavelength absorption maximum.

<sup>2)</sup> Only the effects of *meta*- and *para*-substituents on *meso*-phenyl rings on the redox potentials of *meso*-tetraphenylporphyrins and metalated derivatives have been studied extensively [24a]. In other work, only the oxidation potentials of octaethylporphyrins with CN or NO<sub>2</sub> groups in the *meso*-positions have been determined [24b].



The stationary voltammograms of the dimeric porphyrin **2** displayed broad redox waves with slopes of 100–200 mV (*Table 2*). The broadness of these waves is explained by the presence of two one-electron transfer steps separated by *ca.* 100–130 mV for each of the observed redox waves. The individual electron transfers at each of the two porphyrin sites were best observed for the first oxidation, although the resolution of these waves (slope of 200 mV) only allowed an estimation of the individual redox potentials at +0.25 and +0.45 V *vs.* Fc/Fc<sup>+</sup>. These estimated potentials were in good agreement with values measured by cyclic voltammetry. The results are characteristic of a significant electronic communication between the two porphyrins across the DEE bridge. In other words, oxidation of one macrocycle renders oxidation of the second more difficult. If the two porphyrins were independent of one another, well-defined redox waves of greater amplitude, corresponding to a two-electron redox step, would be expected.

In contrast to the trend observed upon successive attachment of DEE substituents in the series **5**·**Zn**, **9**, and **1**, the first reduction step of dimeric **2** is no longer anodically shifted and occurs at the same potential as the first reduction of **1**. On the other hand, the first oxidation of **2** is facilitated by 110 mV as compared to **1**. Correspondingly, the electrochemical gap in **2** is lowered to 1.75 V (from 1.86 V in **1**). Again, this energy gap is in good agreement with the HOMO-LUMO gap approximated by the maximum of the longest-wavelength absorption. No electrochemical studies were carried out with trimeric **3** due to the small quantities of pure compound that were isolated.

**3. Conclusions.** – A series of soluble, linear porphyrin-DEE arrays (**1**–**3**) ranging from 23 to 53 Å in length was prepared *via* Pd-catalyzed cross-coupling between *meso*-iodo-substituted Zn<sup>II</sup>-porphyrins and (*E*)-1,2-diethynylethenes (DEEs). The electronic absorption spectra provided evidence for efficient  $\pi$ -electron delocalization between DEE and porphyrin subunits. Thus, addition of one or two DEE moieties to porphyrin **5**·**Zn** to give **9** and **1**, respectively, led to strong bathochromic shifts of both *Soret* and *Q* bands. A further substantial bathochromic shift of the *Q* bands was observed upon changing from monoporphyrin **1** to dimeric **2**, in which two macrocycles are linked by a hex-3-ene-1,5-diyne-1,6-diyl bridge. In contrast, the *Soret* band in **2** was no longer shifted but became broadened, displaying a shoulder on the lower-energy edge due to excitonic coupling. The UV/VIS spectrum of **3**, with three porphyrins linked together by hex-3-ene-1,5-diyne-1,6-diyl bridges, resembles the spectrum of **2** which indicates that saturation of the optical properties in these linearly conjugated arrays is already reached at the stage of the dimeric rod.

The electrochemical investigations by stationary voltammetry demonstrated the strong electron-withdrawing character of DEE substituents. Upon increasing the number of DEEs in the series from **5**·**Zn** to **9** and **1**, the first reduction step became anodically shifted by 190 and 350 mV, respectively, whereas the potential for the first oxidation step remained nearly constant. In contrast, upon increasing the rod size by changing from **1** to **2**, the first oxidation step became facilitated, whereas the first reduction step remained at an identical potential. Large differences in the potentials for one-electron oxidation of the two porphyrin moieties in **2** ( $\Delta E = 200$  mV) confirmed the electronic communication between the two macrocycles across the DEE bridge.

This investigation provides another powerful demonstration of the versatility of DEEs such as **7** or **11**. The appended (*t*-Bu)Me<sub>2</sub>SiOCH<sub>2</sub> side chains in these building blocks provide exceptionally high stability and solubility. DEEs not only represent versatile building blocks for the construction of oligomeric and polymeric rods [11][12][25] but also serve as efficient  $\pi$ -conjugative linkers for hybrid materials such as the porphyrin arrays described here. Finally, this study has clearly revealed their strong electron acceptor capacity.

### Experimental Part

*General.* Reagents and solvents of reagent-grade were purchased and used without further purification. Anhyd. MgSO<sub>4</sub> was used as the drying agent after aq. workup. Evaporation and concentration *in vacuo* were carried out at H<sub>2</sub>O-aspirator pressure. Drying *in vacuo* occurred at 10<sup>-2</sup> Torr. Column chromatography (CC): SiO<sub>2</sub> or SiO<sub>2</sub>-H (5–40  $\mu$ m) from *Fluka*. Gel-permeation chromatography (GPC): *Bio-Beads*<sup>®</sup> *SX-1* beads from *Bio-Rad Laboratories*. Prep. TLC: glass sheets coated with 2 mm of SiO<sub>2</sub>-60 F<sub>254</sub> from *E. Merck*. M.p.: *Büchi SMP-20*, uncorrected. Differential scanning calorimetry (DSC): *Dupont 900 Differential Thermal Analyzer*. UV/VIS Spectra ( $\lambda_{\text{max}}$  [nm];  $\epsilon$  [M<sup>-1</sup> cm<sup>-1</sup>]): *Varian Cary-5*, at r.t. IR Spectra [cm<sup>-1</sup>]: *Perkin Elmer-1600-FTIR*. <sup>1</sup>H- and <sup>13</sup>C-NMR spectra: *Bruker-AMX-500*, *Varian Gemini 200* and *300*, at r.t.; with solvent peaks as internal reference. MS (*m/z* (%)): EI (70 eV): *VG-Tribrid* spectrometer; FAB: *VG-ZAB-2SEQ* instrument with a 3-nitrobenzyl-alcohol matrix; MALDI-TOF: *Bruker-Reflex* spectrometer with reflectron detection (positive- or negative-ion mode, acceleration voltage 20 kV) in 3-(3-indolyl)acrylic acid as matrix. Elemental analyses were performed by the Mikrolabor at the Laboratorium für Organische Chemie, ETH-Zürich.

*Electrochemistry Measurements.* The electrochemical measurements were carried out at 20° ± 2° in CH<sub>2</sub>Cl<sub>2</sub> containing 0.1M Bu<sub>4</sub>NPF<sub>6</sub> in a classical three-electrode cell. The electrochemical cell was connected to a computerized multipurpose electrochemical device (*DACFAMOV*, *Microtec-CNRS*, Toulouse, France) interfaced with an *Apple II* microcomputer. The working electrode was a glassy carbon disk electrode used either motionless for CV (10 mV s<sup>-1</sup> to 10 V s<sup>-1</sup>) or as a rotating-disk electrode. The auxiliary electrode was a Pt wire, and a Ag wire was used as a pseudo reference electrode. All potentials are referenced to the ferrocene/ferrocenium (Fc/Fc<sup>+</sup>) couple which was used as an internal standard. The accessible range of potentials was +1.2 to -2.2 V vs. Fc/Fc<sup>+</sup> on glassy carbon in CH<sub>2</sub>Cl<sub>2</sub>. CH<sub>2</sub>Cl<sub>2</sub> was purchased spectroscopic grade from *Merck*, dried over molecular sieves (4 Å), and stored under Ar prior to use. Bu<sub>4</sub>NPF<sub>6</sub> was purchased electrochemical grade from *Fluka* and used as received.

*Ethyl 4-(4-Formylphenoxy)butanoate (4).* A 60% suspension of NaH in hydrocarbon (4.94 g, 123 mmol) was washed with hexane three times. DMF (75 ml) was added, and the slurry was stirred rapidly, while a soln. of 4-hydroxybenzaldehyde (12.5 g, 103 mmol) in DMF (150 ml) was added slowly. A vigorous evolution of H<sub>2</sub> was observed during the addition. After 10 min, the stirring was stopped, and excess NaH was allowed to settle at the bottom of the flask. This soln. of phenoxide ion was transferred to a soln. of ethyl 4-bromobutanoate (20.0 g, 103 mmol, 14.8 ml) in DMF (200 ml). After stirring at r.t. for 12 h, the mixture was quenched with sat. aq. NH<sub>4</sub>Cl soln. (200 ml), poured into AcOEt (300 ml), and washed with sat. aq. NaCl soln. (7 × 300 ml) to remove the DMF, then with 2M K<sub>2</sub>CO<sub>3</sub> (2 × 100 ml). The org. phase was dried, filtered, and the solvent evaporated *in vacuo*. The resulting yellow oil was purified by CC (SiO<sub>2</sub>; hexane/AcOEt 3:1) to afford **4** (21.1 g, 87%). Colorless oil. IR (neat): 1731s, 1692s, 1601s, 1256s, 1149s. <sup>1</sup>H-NMR (200 MHz, CDCl<sub>3</sub>): 1.23 (*t*, *J* = 7.1, 3 H); 2.06–2.19 (*m*, 2 H); 2.50 (*t*, *J* = 7.5, 2 H); 4.05–4.18 (*m*, 4 H); 6.97 (*d*, *J* = 7.9, 2 H); 7.80 (*d*, *J* = 7.9, 2 H); 9.86 (*s*, 1 H). <sup>13</sup>C-NMR (50.3 MHz, CDCl<sub>3</sub>): 13.93; 24.15; 30.35; 60.33; 66.96; 114.63; 129.83; 131.89; 163.86; 172.98; 190.82. EI-MS: 236.1 (*M*<sup>+</sup>). Anal. calc. for C<sub>13</sub>H<sub>16</sub>O<sub>4</sub> (236.27): C 66.09, H 6.83; found: C 66.13, H 6.86.

(*SP-4-1*)-Diethyl 4,4'-{(21H,23H-Porphine-5,15-diyl)bis[benzene-1,4-diyl(oxy)]}bis(butanoate) (**5**). To a soln. of **4** (810 mg, 3.43 mmol) and di(2-pyrryl)methane (500 mg, 3.42 mmol) in degassed CH<sub>2</sub>Cl<sub>2</sub> (600 ml) was added CF<sub>3</sub>COOH (0.16 ml, 2.1 mmol). The mixture was protected from light and stirred at r.t. for 12 h, after which 2,3-dichloro-5,6-dicyano-1,4-benzoquinone (DDQ; 980 mg, 8.64 mmol) was added and stirring was continued for 20 min. Et<sub>3</sub>N (3 ml) was added to neutralize the acid, and the mixture was filtered over a plug (SiO<sub>2</sub>; CHCl<sub>3</sub>). The purple porphyrin fractions were combined, concentrated, and filtered over a second column (SiO<sub>2</sub>; CHCl<sub>3</sub>) to afford **5** (0.54 g, 44%). Violet solid. M.p. 254–256°. UV/VIS (CHCl<sub>3</sub>): 299(15100), 371 (sh, 23100), 397 (sh, 85100), 410(326000), 479 (sh, 2200), 505(16400), 541(5000), 577(3800), 633(1500). IR: 1726s, 1603m, 1243s, 1174s, 1100s. <sup>1</sup>H-NMR (200 MHz, CDCl<sub>3</sub>): -3.10 (*s*, 2 H); 1.34 (*t*, *J* = 7.0, 6 H); 2.26–2.38

(*m*, 4 H); 2.71 (*t*, *J* = 7.1, 4 H); 4.24 (*q*, *J* = 7.0, 4 H); 4.32 (*t*, *J* = 5.8, 4 H); 7.31 (*d*, *J* = 8.7, 4 H); 8.16 (*d*, *J* = 8.7, 4 H); 9.09 (*d*, *J* = 4.6, 4 H); 9.37 (*d*, *J* = 4.6, 4 H); 10.28 (*s*, 2 H). <sup>13</sup>C-NMR (50.3 MHz, CDCl<sub>3</sub>): 14.25; 24.82; 30.94; 60.53; 67.10; 105.18; 113.12; 118.90; 131.09; 131.60; 133.91; 135.94; 145.18; 147.63; 158.89; 173.50. FAB-MS: 723.5 (100, *M*<sup>+</sup>). Anal. calc. for C<sub>44</sub>H<sub>42</sub>N<sub>4</sub>O<sub>6</sub>·H<sub>2</sub>O (740.86): C 71.33, H 5.99, N 7.56; found: C 71.54, H 5.82, N 7.44.

(SP-4-1)-[[Diethyl 4,4'-[(Porphine-5,15-diyl)bis(benzene-1,4-diyl(oxy))]bis(butanoato)](2-)-N<sup>21</sup>,N<sup>22</sup>,N<sup>23</sup>,N<sup>24</sup>]zinc (**5·Zn**). A soln. of **5** (20 mg, 28 μmol) and Zn(OAc)<sub>2</sub>·2 H<sub>2</sub>O (61 mg, 0.28 mmol) in CHCl<sub>3</sub> (20 ml) and MeOH (5 ml) was heated to reflux for 2 h. The pink soln. was washed (H<sub>2</sub>O), dried, filtered, and concentrated *in vacuo*. Filtration over a short plug (SiO<sub>2</sub>; CH<sub>2</sub>Cl<sub>2</sub>) afforded **5·Zn** (20 mg, 92%). M.p. > 250°. UV/VIS (CHCl<sub>3</sub>): 307 (13800), 347 (9500), 414 (439100), 479 (sh, 1000), 508 (sh, 2500), 543 (17600), 580 (2800). IR (CHCl<sub>3</sub>): 1727s, 1603s, 1244s, 1175s. <sup>1</sup>H-NMR (200 MHz, CDCl<sub>3</sub>): 1.32 (*t*, *J* = 7.0, 6 H); 2.24–2.37 (*m*, 4 H); 2.69 (*t*, *J* = 7.2, 4 H); 4.22 (*q*, *J* = 7.0, 4 H); 4.31 (*t*, *J* = 6.2, 4 H); 7.28 (*d*, *J* = 8.7, 4 H); 8.13 (*d*, *J* = 8.7, 4 H); 9.13 (*d*, *J* = 4.6, 4 H); 9.40 (*d*, *J* = 4.6, 4 H); 10.27 (*s*, 2 H). <sup>13</sup>C-NMR (125 MHz, CDCl<sub>3</sub>): 14.25; 24.85; 30.97; 60.53; 67.13; 106.23; 112.39; 113.84; 131.75; 132.64; 135.18; 135.72; 149.56; 150.61; 158.74; 173.53. FAB-MS: 784.3 (100, *M*<sup>+</sup>). Anal. calc. for C<sub>44</sub>H<sub>40</sub>N<sub>4</sub>O<sub>6</sub>Zn (786.21): C 67.22, H 5.13, N 7.13; found: C 67.18, H 5.15, N 7.26.

(SP-4-1)-Diethyl 4,4'-[(10,20-Diiodo-21H,23H-porphine-5,15-diyl)bis(benzene-1,4-diyl(oxy))]bis(butanoate) (**6**). To a light-protected soln. of (AcO)<sub>2</sub>I<sub>2</sub>Ph (293 mg, 0.681 mmol) in CHCl<sub>3</sub> (30 ml) was added a soln. of I<sub>2</sub> (149 mg, 0.587 mmol) in CHCl<sub>3</sub> (20 ml). Pyridine (15 pipette drops) was then added to the above red-violet soln., causing decoloration to light yellow within 15 min. This mixture was then added dropwise over 45 min to a stirred soln. of **5** (0.34 g, 0.47 mmol) in CHCl<sub>3</sub> (340 ml). After 1 h, the soln. was washed with sat. aq. Na<sub>2</sub>S<sub>2</sub>O<sub>3</sub> soln. (2 × 100 ml), dried, and filtered. The volume was reduced *in vacuo*, and Et<sub>2</sub>O was added to precipitate the deep-violet product which was collected, washed (Et<sub>2</sub>O), and dried *in vacuo* to yield **6** (415 mg, 90%). If necessary, the product was further purified by CC (SiO<sub>2</sub>; CH<sub>2</sub>Cl<sub>2</sub>/hexane 10:1). M.p. 214–215°. UV/VIS (CHCl<sub>3</sub>): 381 (sh, 20300), 427 (311000), 495 (4200), 527 (13200), 564 (13100), 605 (4500), 663 (6100). IR (CCl<sub>4</sub>): 1736s, 1653w, 1607w, 1600w, 1506m, 1247s, 1176s. <sup>1</sup>H-NMR (500 MHz, Cl<sub>2</sub>DCCDCDCl<sub>2</sub>): –2.73 (*s*, 2 H); 1.28 (*t*, *J* = 7.1, 6 H); 2.22–2.28 (*m*, 4 H); 2.63 (*t*, *J* = 7.3, 4 H); 4.16 (*q*, *J* = 7.1, 4 H); 4.25 (*t*, *J* = 6.0, 4 H); 7.22 (*d*, *J* = 8.4, 4 H); 7.97 (*d*, *J* = 8.4, 4 H); 8.77 (*d*, *J* = 4.7, 4 H); 9.53 (*d*, *J* = 4.7, 4 H). FAB-MS: 975.1 (100, *M*<sup>+</sup>). Anal. calc. for C<sub>44</sub>H<sub>40</sub>I<sub>2</sub>N<sub>4</sub>O<sub>6</sub>·H<sub>2</sub>O (992.66): C 53.24, H 4.26, N 5.64; found: C 53.47, H 4.14, N 5.66.

(SP-4-1)-[[Diethyl 4,4'-[(10,20-Diiodoporphine-5,15-diyl)bis(benzene-1,4-diyl(oxy))]bis(butanoato)](2-)-N<sup>21</sup>,N<sup>22</sup>,N<sup>23</sup>,N<sup>24</sup>]zinc (**6·Zn**). A violet mixture of **6** (157 mg, 0.161 mmol) and Zn(OAc)<sub>2</sub>·2 H<sub>2</sub>O (329 mg, 1.50 mmol) in THF/CHCl<sub>3</sub>/MeOH (120 ml/20 ml/15 ml) was heated to reflux for 3 h, after which time the soln. was deep blue-green. Evaporation *in vacuo* and dissolution of the crude product in THF, precipitation with MeOH, filtration, washing of the solid with MeOH, and drying *in vacuo* afforded **6·Zn** (139 mg, 83%) as a metallic-violet solid. If necessary, the product was further purified by filtration over a short column (SiO<sub>2</sub>; THF/CHCl<sub>3</sub> 1:1). M.p. 226–227°. UV/VIS (CHCl<sub>3</sub>): 316 (24600), 431 (379900), 528 (6500), 566 (14300), 611 (8400), 663 (2000). IR (CCl<sub>4</sub>): 1737s, 1605m, 1508m, 1245s, 1173s. <sup>1</sup>H-NMR (500 MHz, (D<sub>8</sub>)THF): 1.30 (*t*, *J* = 7.1, 6 H); 2.25–2.30 (*m*, 4 H); 2.66 (*t*, *J* = 7.3, 4 H); 4.19 (*q*, *J* = 7.1, 4 H); 4.34 (*t*, *J* = 6.2, 4 H); 7.32 (*d*, *J* = 8.5, 4 H); 8.04 (*d*, *J* = 8.5, 4 H); 8.84 (*d*, *J* = 4.6, 4 H); 9.68 (*d*, *J* = 4.6, 4 H). <sup>13</sup>C-NMR (125.8 MHz, (D<sub>8</sub>)THF): 14.67; peak hidden under THF (at 24.86–26.34); 31.32; 60.71; peak hidden under THF (at 66.91–68.51); 80.50; 113.34; 122.95; 134.08; 135.89; 136.39; 138.27; 152.73; 153.33; 160.00; 173.13. FAB-MS: 1036.1 (100, *M*<sup>+</sup>). Anal. calc. for C<sub>44</sub>H<sub>38</sub>I<sub>2</sub>N<sub>4</sub>O<sub>6</sub>Zn (1038.01): C 50.91, H 3.69, N 5.40; found: C 50.68, H 3.60, N 5.17.

(SP-4-1)-[[Diethyl 4,4'-[[10,20-Bis[(*E*)-3,4-bis[(tert-butyl)dimethylsilyloxy]methyl]-6-(trimethylsilyl)hex-3-ene-1,5-dienyl](porphine-5,15-diyl)bis(benzene-1,4-diyl(oxy))]bis(butanoato)](2-)-N<sup>21</sup>,N<sup>22</sup>,N<sup>23</sup>,N<sup>24</sup>]zinc (**1**). To a degassed soln. of Et<sub>3</sub>N (20 μl, 0.14 mmol) in dry THF (5 ml) were added **6·Zn** (20 mg, 19 μmol), **7** (20 mg, 46 μmol), [Pd<sub>2</sub>(dba)<sub>3</sub>] (5 mg, 5 μmol), AsPh<sub>3</sub> (4.0 mg, 13 μmol), and CuI (1 mg, 5 μmol). The soln. was stirred under N<sub>2</sub> in the absence of light for 6 h at 45° then for 12 h at r.t. After evaporation *in vacuo*, the crude product was filtered through a plug (SiO<sub>2</sub>; CH<sub>2</sub>Cl<sub>2</sub>). GPC (CH<sub>2</sub>Cl<sub>2</sub>) of the middle fraction separated **1** (19 mg, 60%) from the mixture of **8** and **9**. Prep. TLC (SiO<sub>2</sub>; CH<sub>2</sub>Cl<sub>2</sub>/THF 99.75:0.25) provided pure **8** (higher R<sub>f</sub>; 1.5 mg, 6%) and **9** (lower R<sub>f</sub>; 1.5 mg, 6%).

*Data of 1*: Emerald-green solid. DSC: 178° (dec.). UV/VIS (CHCl<sub>3</sub>): 260 (30700), 330 (27100), 458 (426100), 560 (sh, 4900), 596 (sh, 9400), 624 (sh, 14800), 673 (70100). IR (CHCl<sub>3</sub>): 2128w, 1727m, 1603s, 1251m, 1175m. <sup>1</sup>H-NMR (200 MHz, CDCl<sub>3</sub>): 0.26 (*s*, 12 H); 0.29 (*s*, 18 H); 0.30 (*s*, 12 H); 1.00 (*s*, 18 H); 1.29 (*t*, *J* = 7.2, 6 H); 2.16–2.29 (*m*, 4 H); 2.61 (*t*, *J* = 7.0, 4 H); 4.10 (*q*, *J* = 7.2, 4 H); 4.25 (*t*, *J* = 5.8, 4 H); 4.97 (*s*, 4 H); 5.05 (*s*, 4 H); 7.27 (*d* partially hidden by CHCl<sub>3</sub> peak at 7.24, 4 H); 8.06 (*d*, *J* = 8.3, 4 H); 8.86 (*d*, *J* = 4.6, 4 H); 9.74 (*d*, *J* = 4.6, 4 H). <sup>13</sup>C-NMR (125.8 MHz, CDCl<sub>3</sub>): –4.83; –4.76; –0.04; 14.13; 18.58; 18.69; 24.58; 26.06; 26.22; 30.62; 60.38; 64.67; 65.14; 66.79; 94.52; 101.60; 102.60; 105.10; 107.21; 112.74; 122.88;

129.10; 131.21; 131.81; 132.67; 134.54; 135.46; 150.52; 151.95; 158.63; 173.11. FAB-MS: 1654.6 (100,  $M^+$ ,  $^{12}C_{90}H_{124}N_4O_{10}Si_6^{66}Zn^+$ ). Anal. calc. for  $C_{90}H_{124}N_4O_{10}Si_6Zn \cdot 2 H_2O$  (1691.94): C 63.89, H 7.63, N 3.31; found: C 63.72, H 7.52, N 3.31.

(SP-4-1)-[[Diethyl 4,4'-[[10-[[[(E)-3,4-Bis[[tert-butyl]dimethylsilyloxy]methyl]-6-(trimethylsilyl)hex-3-ene-1,5-diynyl]](porphine-5,15-diyl)]bis[benzene-1,4-diyl(oxy)]]bis(butanoato)](2-)-N<sup>21</sup>,N<sup>22</sup>,N<sup>23</sup>,N<sup>24</sup>]zinc (**8**). Blue-green solid. M.p. 192°. DSC: 201° (dec.). UV/VIS (CHCl<sub>3</sub>): 323 (22500), 448 (357100), 545 (sh, 5200), 578 (12400), 642 (34200). IR (CHCl<sub>3</sub>): 2133w, 1729s, 1604m, 1246s, 1215s, 1175m. <sup>1</sup>H-NMR (500 MHz, CDCl<sub>3</sub>): 0.26 (s, 6 H); 0.29 (s, 9 H); 0.31 (s, 6 H); 1.02 (s, 9 H); 1.03 (s, 9 H); 1.21 (t,  $J = 7.1$ , 6 H); 2.05–2.09 (m, 4 H); 2.48 (t,  $J = 7.1$ , 4 H); 3.94 (q,  $J = 7.1$ , 4 H); 4.12 (t,  $J = 6.0$ , 4 H); 4.96 (s, 2 H); 5.04 (s, 2 H); 7.21 (d,  $J = 8.5$ , 4 H); 8.01 (d,  $J = 8.5$ , 4 H); 8.83 (d,  $J = 4.6$ , 2 H); 8.86 (d,  $J = 4.6$ , 2 H); 9.63 (d,  $J = 4.6$ , 2 H); 9.71 (d,  $J = 4.6$ , 2 H). <sup>13</sup>C-NMR (125.8 MHz, CDCl<sub>3</sub>): –4.83; –4.77; –0.04; 14.21; 18.57; 18.68; 24.72; 26.05; 26.21; 30.78; 60.44; 64.66; 65.12; 66.97; 83.16; 96.14; 100.89; 102.63; 104.90; 107.20; 112.74; 122.54; 129.05; 131.49; 131.81; 133.05; 133.37; 134.51; 135.46; 137.80; 150.49; 151.82; 151.96; 152.63; 158.70; 173.16. FAB-MS: 1346.5 (100,  $M^+$ ,  $^{12}C_{67}H_{81}IN_4O_8Si_3^{66}Zn^+$ ), 1218.5 (30,  $[M-I]^+$ ). Anal. calc. for  $C_{67}H_{81}IN_4O_8Si_3Zn$  (1346.95): C 59.75, H 6.06, N 4.16; found: C 59.47, H 5.81, N 3.95.

(SP-4-1)-[[Diethyl 4,4'-[[10-[[[(E)-3,4-Bis[[tert-butyl]dimethylsilyloxy]methyl]-6-(trimethylsilyl)hex-3-ene-1,5-diynyl]](porphine-5,15-diyl)]bis[benzene-1,4-diyl(oxy)]]bis(butanoato)](2-)-N<sup>21</sup>,N<sup>22</sup>,N<sup>23</sup>,N<sup>24</sup>]zinc (**9**). Blue-green solid. DSC: 210° (dec.). UV/VIS (CHCl<sub>3</sub>): 315 (18200), 349 (sh, 16200), 369 (sh, 14700), 445 (277800), 535 (sh, 4000), 572 (11600), 625 (20200). IR (CHCl<sub>3</sub>): 2128w, 1717m, 1605m, 1260s, 1248s, 1174s. <sup>1</sup>H-NMR (200 MHz, CDCl<sub>3</sub>): 0.26 (s, 6 H); 0.28 (s, 9 H); 0.30 (s, 6 H); 1.01 (s, 9 H); 1.04 (s, 9 H); 1.29 (t,  $J = 7.3$ , 6 H); 2.12–2.31 (m, 4 H); 2.63 (t,  $J = 7.2$ , 4 H); 4.13 (q,  $J = 7.3$ , 4 H); 4.26 (t,  $J = 6.0$ , 4 H); 4.98 (s, 2 H); 5.08 (s, 2 H); 7.23 (d,  $J = 8.9$ , 4 H); 8.08 (d,  $J = 8.9$ , 4 H); 8.97 (d,  $J = 4.7$ , 2 H); 8.99 (d,  $J = 4.7$ , 2 H); 9.22 (d,  $J = 5.0$ , 2 H); 9.83 (d,  $J = 5.0$ , 2 H); 10.15 (s, 1 H). <sup>13</sup>C-NMR (125.8 MHz, CDCl<sub>3</sub>): –4.83; –4.76; –0.03; 14.29; 18.59; 18.71; 24.87; 26.07; 26.23; 30.97; 60.51; 64.69; 65.19; 67.08; 94.04; 100.22; 102.66; 105.30; 106.99; 107.59; 112.78; 121.39; 128.84; 131.14; 131.78; 131.91; 132.46; 132.72; 134.76; 135.52; 149.43; 150.15; 150.94; 151.95; 158.66; 173.29. FAB-MS:  $m/z$  calc. 1218.4 (100,  $M^+$ ). HR-FAB-MS: 1218.4711 ( $M^+$ ,  $^{12}C_{67}H_{82}N_4O_8Si_3^{66}Zn^+$ ; calc. 1218.4732).

(SP-4-1)-[[Diethyl 4,4'-[[10,20-Bis[[[(E)-3,4-bis[[tert-butyl]dimethylsilyloxy]methyl]hex-3-ene-1,5-diynyl]](porphine-5,15-diyl)]bis[benzene-1,4-diyl(oxy)]]bis(butanoato)](2-)-N<sup>21</sup>,N<sup>22</sup>,N<sup>23</sup>,N<sup>24</sup>]zinc (**10**). An aq. soln. of AgNO<sub>3</sub> (104 mg, 0.612 mmol in H<sub>2</sub>O (2 ml)) was carefully added to a soln. of **1** (188 mg, 0.114 mmol) in acetone (30 ml) and THF (5 ml). A fine solid precipitated within several min. The mixture was stirred at r.t. for 2 h in the absence of light, then aq. KCN (186 mg, 2.86 mmol in H<sub>2</sub>O (2 ml)) was added, and the mixture was stirred for 2 h, after which time all of the precipitate had dissolved. After concentration *in vacuo*, CH<sub>2</sub>Cl<sub>2</sub> (50 ml) was added, and the soln. was washed with sat. aq. NH<sub>4</sub>Cl soln. The aq. phase was washed with CH<sub>2</sub>Cl<sub>2</sub> and the combined org. layers were dried, filtered, and evaporated *in vacuo*. Filtration over a short plug (SiO<sub>2</sub>; CH<sub>2</sub>Cl<sub>2</sub>, then THF) afforded **10** (146 mg, 85%). Deep-green solid. M.p. 187° (dec.). UV/VIS (CHCl<sub>3</sub>): 304 (sh, 22000), 329 (24400), 454 (321200), 547 (5600), 596 (sh, 9700), 667 (50100). IR (CHCl<sub>3</sub>): 2400w, 2178w, 1724m, 1606m, 1250s, 1174m, 1094w. <sup>1</sup>H-NMR (200 MHz, CDCl<sub>3</sub>): 0.23 (s, 12 H); 0.28 (s, 12 H); 0.99 (s, 18 H); 1.01 (s, 18 H); 1.30 (t,  $J = 7.0$ , 6 H); 2.18–2.33 (m, 4 H); 2.64 (t,  $J = 7.5$ , 4 H); 3.69 (s, 2 H); 4.15 (q,  $J = 7.0$ , 4 H); 4.28 (t,  $J = 6.2$ , 4 H); 4.95 (s, 4 H); 5.06 (s, 4 H); 7.26 (d,  $J = 8.7$ , 4 H); 8.06 (d,  $J = 8.7$ , 4 H); 8.87 (d,  $J = 4.2$ , 4 H); 9.72 (d,  $J = 4.2$ , 4 H). <sup>13</sup>C-NMR (125 MHz, CDCl<sub>3</sub>): –4.86; –4.81; 14.30; 18.55; 18.65; 24.89; 26.01; 26.15; 30.98; 60.54; 64.72; 64.95; 67.07; 81.27; 88.98; 94.09; 101.56; 104.80; 112.81; 122.96; 128.16; 131.31; 132.54; 132.77; 134.48; 135.44; 150.62; 151.98; 158.75; 173.31. FAB-MS: 1510.4 (100,  $M^+$ ,  $^{12}C_{84}H_{108}N_4O_{10}Si_4^{66}Zn$ ). Anal. calc. for  $C_{84}H_{108}N_4O_{10}Si_4Zn \cdot CH_2Cl_2$  (1596.47): C 63.95, H 6.95, N 3.51; found: C 63.98, H 6.91, N 3.28.

(SP-4-1)-[[Tetraethyl 4,4'-[[[(E)-3,4-Bis[[tert-butyl]dimethylsilyloxy]methyl]hex-3-ene-1,5-diyne-1,6-diyl]]bis[[20-[[[(E)-3,4-bis[[tert-butyl]dimethylsilyloxy]methyl]-6-(trimethylsilyl)hex-3-ene-1,5-diynyl]](porphine-10,5,15-triyl)]bis[benzene-1,4-diyl(oxy)]]tetrakis(butanoato)](4-)-N<sup>21</sup>,N<sup>22</sup>,N<sup>23</sup>,N<sup>24</sup>]zinc (**2**). To a degassed soln. of **8** (50 mg, 37 μmol), [Pd<sub>2</sub>(dba)<sub>3</sub>] (5.0 mg, 5.5 μmol), AsPh<sub>3</sub> (2.0 mg, 6.5 μmol), and CuI (1.0 mg, 5.3 μmol) in dry THF (15 ml), containing one pipette drop of HN(i-Pr)<sub>2</sub>, was added **11** (6.0 mg, 16 μmol). The soln. was heated to 40° for 6 h then stirred at r.t. for 18 h. After evaporation *in vacuo*, the residue was filtered through a plug (SiO<sub>2</sub>; CH<sub>2</sub>Cl<sub>2</sub>), subjected to GPC (THF, 80-cm column), and then the fractions enriched in product were purified by CC (SiO<sub>2</sub>; CH<sub>2</sub>Cl<sub>2</sub> containing 0–1% THF) to afford **2** (11 mg, 24%). Brown-green solid. M.p. >250°. UV/VIS (CHCl<sub>3</sub>): 261 (46300), 332 (42200), 460 (156600), 511 (sh, 56600), 591 (18600), 650 (sh, 38100), 696 (66900), 726 (69100). IR (CHCl<sub>3</sub>): 2178w, 2129w, 1728m, 1606m, 1250s, 1174m, 1093m, 1044m. <sup>1</sup>H-NMR (200 MHz, CDCl<sub>3</sub>): 0.27 (s, 12 H); 0.29 (s, 12 H); 0.30 (s, 18 H); 0.43 (s, 12 H); 1.02 (s, 36 H); 1.06 (s, 18 H); 1.22 (t,  $J = 7.1$ , 12 H); 2.07–2.18 (m, 8 H); 2.53 (t,  $J = 7.5$ , 8 H); 3.93 (q,  $J = 7.1$ , 8 H); 4.17 (t,  $J = 5.0$ , 8 H); 4.95

(s, 4 H); 4.97 (s, 4 H); 5.49 (s, 4 H); 7.30 (d,  $J=8.3$ , 8 H); 8.09 (d,  $J=8.3$ , 8 H); 8.74 (d,  $J=4.6$ , 4 H); 8.80 (d,  $J=5.0$ , 4 H); 9.37–9.40 (br. m, 4 H); 9.55–9.58 (br. m, 4 H).  $^{13}\text{C-NMR}$  (125.8 MHz,  $\text{CDCl}_3$ ): –4.80; –4.76; –4.45; 0.01; 14.27; 18.57; 18.68; 18.74; 24.89; 26.08; 26.23; 26.26; 30.92; 60.49; 64.67; 65.15; 65.82; 67.08; 94.44; 95.74; 101.24; 101.61; 102.80; 104.81; 105.83; 107.07; 122.04; 122.88; 128.85; 129.02; 129.98; 130.83; 130.91; 131.70; 132.46; 134.65; 135.48; 135.70; 150.34; 150.39; 151.65; 158.75; 173.22. FAB-MS: 2802.2 (100,  $M^+$ ,  $^{13}\text{C}_{153}\text{H}_{196}\text{N}_8\text{O}_{18}\text{Si}_8\text{Zn}^{68}\text{Zn}^{64}$ ). MALDI-TOF: 2804.3 (100,  $M^+$ ).

(SP-4-I)-[[Hexaethyl 4,4'-[[Bis[[[10-(E)-3,4-bis[[tert-butyl]dimethylsilyloxy]methyl]hex-3-ene, 1,5-diyne-1,6-diyl]-20-(E)-(3,4-bis[[tert-butyl]dimethylsilyloxy]methyl]-6-(trimethylsilyl)hex-3-ene-1,5-diyne]](porphine-5,15-diyl)]bis[benzene-1,4-diyl(oxy)]]porphine-10,20,5,15-tetrayl]bis[benzene-1,4-diyl(oxy)]]hexakis(butanoato)](6-)- $\text{N}^{21}\text{N}^{22}\text{N}^{23}\text{N}^{24}$ zinc (**3**). To a degassed soln. of **10** (30 mg, 20  $\mu\text{mol}$ ) were added **8** (53 mg, 40  $\mu\text{mol}$ ),  $[\text{Pd}_2(\text{dba})_3]$  (5.0 mg, 5.5  $\mu\text{mol}$ ), and  $\text{AsPh}_3$  (3.0 mg, 9.8  $\mu\text{mol}$ ) in dry THF (2 ml) containing  $\text{Et}_3\text{N}$  (0.1 ml) as well as  $\text{CuI}$  (2 mg, 0.1 mmol). The green soln. was stirred at r.t. for 22 h in the absence of light. After evaporation *in vacuo*, the residue was filtered through  $\text{SiO}_2$  ( $\text{CH}_2\text{Cl}_2$  containing 0–50% THF). The product fractions obtained upon elution with  $\text{CH}_2\text{Cl}_2$  were washed with sat. aq.  $\text{NH}_4\text{Cl}$  soln. and dried ( $\text{Na}_2\text{SO}_4$ ). GPC ( $\text{CH}_2\text{Cl}_2$ ; 160-cm column) provided **3** (5 mg, 6%). Brown-green solid. M.p. >250°; UV/VIS ( $\text{CHCl}_3$ ): 256 (62900), 308 (sh, 57700), 330 (62300), 457 (315300), 496 (sh, 150000), 588 (26800), 730 (111800). IR ( $\text{CCl}_4$ ): 2178w, 2130w, 1737m, 1731m, 1712m, 1606m, 1248s, 1175m, 1094m.  $^1\text{H-NMR}$  (500 MHz,  $\text{CDCl}_3$ ): 0.20 (s, 24 H); 0.21 (s, 12 H); 0.24 (s, 18 H); 0.40 (s, 12 H); 0.95 (s, 18 H); 0.96 (s, 18 H); 0.98 (s, 18 H); 1.02 (s, 18 H); 1.26–1.31 (m, 18 H); 2.25–2.29 (m, 12 H); 2.64–2.67 (m, 12 H); 4.16–4.20 (m, 12 H); 4.27–4.29 (m, 12 H); 4.90 (s, 4 H); 5.00 (s, 4 H); 5.55 (s, 8 H); 7.23–7.24 (m, 12 H); 8.04 (d,  $J=7.7$ , 8 H); 8.11 (d,  $J=8.5$ , 4 H); 8.73 (d,  $J=4.4$ , 4 H); 8.79–8.81 (m, 8 H); 9.59 (d,  $J=4.5$ , 4 H); 9.74–9.76 (m, 8 H).  $^{13}\text{C-NMR}$  (125 MHz,  $\text{CDCl}_3$ ): –5.07; –5.00; –4.69; –0.27; 14.09; 18.23; 18.43; 18.54; 18.64; 24.78; 25.85; 25.90; 26.02; 26.08; 30.98; 60.60; 64.54; 65.03; 65.73; 66.96; 86.97; 105.89; 106.95; 112.49; 122.65; 130.72; 130.85; 131.72; 132.27; 134.96; 135.36; 150.34; 151.81; 151.88; 158.39; 173.70. MALDI-TOF: 3950.6 (100,  $M^+$ ; calc. for  $^{13}\text{C}_{216}\text{H}_{268}\text{N}_{12}\text{O}_{26}\text{Si}_{10}\text{Zn}^{68}\text{Zn}^{66}\text{Zn}^{64}$ : 3949.6).

This work was supported by the *ETH Research Council (TEMA grant)*. We thank Dr. Harry Anderson (Oxford University) and Dr. Christiane Dietrich-Buchecker (Université Louis Pasteur, Strasbourg) for helpful discussions, and Dr. Carlo Thilgen for his assistance with the nomenclature.

## REFERENCES

- [1] 'Electronic Materials: The Oligomer Approach', Eds. K. Müllen and G. Wegner, Wiley-VCH, Weinheim, 1997.
- [2] a) J. M. Tour, *Chem. Rev.* **1996**, *96*, 537; b) J. Roncali, *ibid.* **1997**, *97*, 173.
- [3] a) V. S.-Y. Lin, S. G. DiMagno, M. J. Therien, *Science (Washington, D.C.)* **1994**, *264*, 1105; b) V. S.-Y. Lin, M. J. Therien, *Chem. Eur. J.* **1995**, *1*, 645.
- [4] For recent examples, see: O. Mongin, C. Papamicaël, N. Hoyler, A. Gossauer, *J. Org. Chem.* **1998**, *63*, 5568; K. Sugiura, G. Ponomarev, S. Okubo, A. Tajiri, Y. Sakata, *Bull. Chem. Soc. Jpn.* **1997**, *70*, 1115; S. Kawabata, I. Yamazaki, Y. Nishimura, A. Osuka, *J. Chem. Soc., Perkin Trans. 2* **1997**, 479; A. Osuka, H. Shimidzu, *Angew. Chem.* **1997**, *109*, 93; *ibid.*, *Int. Ed. Engl.* **1997**, *36*, 135; F. Li, S. Gentemann, W. A. Kalsbeck, J. Seth, J. S. Lindsey, D. Holten, D. F. Bocian, *J. Mater. Chem.* **1997**, *7*, 1245; P. J. F. de Rege, M. J. Therien, *Inorg. Chim. Acta* **1996**, *242*, 211; R. W. Wagner, T. E. Johnson, J. S. Lindsey, *J. Am. Chem. Soc.* **1996**, *118*, 11166; J.-S. Hsiao, B. P. Krueger, R. W. Wagner, T. E. Johnson, J. K. Delaney, D. C. Mauzerall, G. R. Fleming, J. S. Lindsey, D. F. Bocian, R. J. Donohoe, *ibid.* **1996**, *118*, 11181; A. Osuka, N. Tanabe, S. Kawabata, I. Yamazaki, Y. Nishimura, *J. Org. Chem.* **1995**, *60*, 7177; A. K. Burrell, D. L. Officer, D. C. W. Reid, *Angew. Chem.* **1995**, *107*, 986; *ibid.*, *Int. Ed. Engl.* **1995**, *34*, 900; J. L. Sessler, V. L. Capuano, A. Harriman, *J. Am. Chem. Soc.* **1993**, *115*, 4618; E. J. Atkinson, A. M. Oliver, M. N. Padon-Row, *Tetrahedron Lett.* **1993**, *34*, 6147.
- [5] a) P. N. Taylor, A. P. Wylie, J. Huuskonen, H. L. Anderson, *Angew. Chem.* **1998**, *110*, 1033; *ibid.*, *Int. Ed. Engl.* **1998**, *37*, 986; b) D. P. Arnold, D. A. James, *J. Org. Chem.* **1997**, *62*, 3460; c) B. Jiang, W. E. Jones, Jr., *Macromolecules* **1997**, *30*, 5575; J. R. Reimers, T. X. Lü, M. J. Crossley, N. S. Hush, *Nanotechnology* **1996**, *7*, 424; d) H. Higuchi, M. Takeuchi, J. Ojima, *Chem. Lett.* **1996**, 593.
- [6] a) R. W. Wagner, J. Seth, S. I. Yang, D. Kim, D. F. Bocian, D. Holten, J. S. Lindsey, *J. Org. Chem.* **1998**, *63*, 5042; b) B. Jiang, S.-W. Yang, D. C. Barbini, W. E. Jones, Jr., *Chem. Commun.* **1998**, 213; c) R. Stranger, J. E. McGrady, D. P. Arnold, G. A. Heath, *Inorg. Chem.* **1996**, *35*, 7791; d) J. J. Gosper, M. Ali, *J. Chem. Soc., Chem. Commun.* **1994**, 1707; e) D. P. Arnold, G. A. Heath, *J. Am. Chem. Soc.* **1993**, *115*, 12197.

- [7] a) H. L. Anderson, *Inorg. Chem.* **1994**, *33*, 972; b) H. L. Anderson, S. J. Martin, D. D. C. Bradley, *Angew. Chem.* **1994**, *106*, 711; *ibid.*, *Int. Ed. Engl.* **1994**, *33*, 655.
- [8] R. W. Wagner, J. S. Lindsey, *J. Am. Chem. Soc.* **1994**, *116*, 9759.
- [9] D. Beljonne, G. E. O'Keefe, P. J. Hamer, R. H. Friend, H. L. Anderson, J. L. Brédas, *J. Chem. Phys.* **1997**, *106*, 9439.
- [10] R. W. Wagner, J. S. Lindsey, J. Seth, V. Palaniappan, D. F. Bocian, *J. Am. Chem. Soc.* **1996**, *118*, 3996.
- [11] R. E. Martin, U. Gubler, C. Boudon, V. Gramlich, C. Bosshard, J.-P. Gisselbrecht, P. Günter, M. Gross, F. Diederich, *Chem. Eur. J.* **1997**, *3*, 1505.
- [12] M. Schreiber, J. Anthony, F. Diederich, M. E. Spahr, R. Nesper, M. Hubrich, F. Bommeli, L. Degiorgi, P. Wachter, P. Kaatz, C. Bosshard, P. Günter, M. Colussi, U. W. Suter, C. Boudon, J.-P. Gisselbrecht, M. Gross, *Adv. Mater.* **1994**, *6*, 786.
- [13] CVFF force field, Insight II, Version 95.0 in Discover 2.9.7, Biosym Technologies, San Diego, 1997.
- [14] a) R. W. Boyle, C. K. Johnson, D. Dolphin, *J. Chem. Soc., Chem. Commun.* **1995**, 527; b) S. M. LeCours, H.-W. Guan, S. G. DiMagno, C. H. Wang, M. J. Therien, *J. Am. Chem. Soc.* **1996**, *118*, 1497; c) S. M. LeCours, S. G. DiMagno, M. J. Therien, *ibid.* **1996**, *118*, 11854; d) D. A. Shultz, K. P. Gwaltney, H. Lee, *J. Org. Chem.* **1998**, *63*, 4034.
- [15] H. L. Anderson, *Tetrahedron Lett.* **1992**, *33*, 1101; G. S. Wilson, H. L. Anderson, *Synlett* **1996**, 1039; L. R. Milgrom, G. Yahiolu, *Tetrahedron Lett.* **1996**, *37*, 4069; L. R. Milgrom, R. D. Rees, G. Yahiolu, *ibid.* **1997**, *38*, 4905; L. R. Milgrom, G. Yahiolu, D. W. Bruce, S. Morrone, F. Z. Henari, W. J. Blau, *Adv. Mater.* **1997**, *9*, 313.
- [16] D. P. Arnold, L. J. Nitschinsk, *Tetrahedron* **1992**, *48*, 8781; D. P. Arnold, A. W. Johnson, M. Mahendran, *J. Chem. Soc., Perkin Trans. 1* **1978**, 366.
- [17] D. R. Buckle, A. E. Fenwick, D. J. Outred, C. J. M. Rockell, *J. Chem. Res. (M)* **1987**, 3144.
- [18] R. Chong, P. S. Clezy, A. J. Liepa, A. W. Nichol, *Austr. J. Chem.* **1969**, *22*, 229.
- [19] J. S. Manka, D. S. Lawrence, *Tetrahedron Lett.* **1989**, *30*, 6989; C.-H. Lee, J. S. Lindsey, *Tetrahedron* **1994**, *50*, 11427.
- [20] R. R. Tykwinski, M. Schreiber, R. Pérez Carlon, F. Diederich, *Helv. Chim. Acta* **1996**, *79*, 2449.
- [21] H. M. Schmidt, J. F. Arens, *Recl. Trav. Chim. Pays-Bas* **1967**, *86*, 1138.
- [22] M. Kasha, H. R. Rawls, M. A. El-Bayoumi, *Pure Appl. Chem.* **1965**, *11*, 371.
- [23] A. Giraudeau, H. J. Callot, J. Jordan, I. Ezhar, M. Gross, *J. Am. Chem. Soc.* **1979**, *101*, 3857; A. Giraudeau, H. J. Callot, M. Gross, *Inorg. Chem.* **1979**, *18*, 201.
- [24] a) K. M. Kadish, M. M. Morrison, *J. Am. Chem. Soc.* **1976**, *98*, 3326; K. M. Kadish, M. M. Morrison, L. A. Constant, L. Dickens, D. G. Davis, *ibid.* **1976**, *98*, 8387; b) E. C. Johnson, D. Dolphin, *Tetrahedron Lett.* **1976**, 2197; H. J. Callot, A. Louati, M. Gross, *Bull. Soc. Chim. Fr.* **1983**, *II*, 317.
- [25] A. P. H. J. Schenning, R. E. Martin, M. Ito, F. Diederich, C. Boudon, J.-P. Gisselbrecht, M. Gross, *Chem. Commun.* **1998**, 1013.

Received August 31, 1998